INVESTIGATING THE WRENCH CAPABILITIES OF A KINEMATICALLY-REDUNDANT PLANAR PARALLEL MANIPULATOR

Roger Boudreau[1], Scott Nokleby[2], Marise Gallant[1]
[1]*Université de Moncton, Moncton, NB*
[2]*University of Ontario Institute of Technology, Oshawa, ON*
Email: roger.a.boudreau@umoncton.ca; scott.nokleby@uoit.ca; marise.gallant@umoncton.ca

ABSTRACT

This paper presents an explicit method to obtain the wrench capabilities of kinematically-redundant planar parallel manipulators using a wrench polytope approach. A methodology proposed by others for non-redundant and actuation-redundant manipulators is adapted to kinematically-redundant manipulators. The fact that the latter type of manipulators have an infinite number of solutions to the inverse kinematics problem would lead one to foresee optimization as the logical method to obtain its force capabilities. The proposed method does not use optimization and is, therefore, exact and very efficient. The methodology applied to a pure-force analysis of an example manipulator at a given pose produced the same results as those obtained by others using optimization.

Keywords: force/moment (wrench) capabilities; kinematic redundancy; planar parallel manipulators.

ÉTUDE DE L'EFFET DE LA REDONDANCE CINÉMATIQUE SUR LA CAPACITÉ DES TORSEURS D'UN MANIPULATEUR PARALLÈLE PLAN

RÉSUMÉ

Cet article présente une méthode pour obtenir explicitement les capacités des torseurs (forces/moments) d'un manipulateur parallèle plan avec redondance cinématique. Une méthodologie développée par d'autres pour des manipulateurs non-redondants et avec redondance d'actionnement est adaptée aux manipulateurs avec redondance cinématique. Le fait que ces derniers possèdent une infinité de solutions au problème géométrique inverse laisse présumer que l'optimisation serait la méthode logique pour obtenir les capacités en force. La méthode proposée ne requiert pas d'optimisation et produit donc une solution exacte et efficace. La méthode appliquée à une analyse en force seulement pour un manipulateur à une pose prescrite a produit les mêmes résultats que ceux obtenus par d'autres en utilisant une méthode d'optimisation.

Mots-clés : capacités forces/moments (torseurs) ; redondance cinématique ; manipulateurs parallèles plans.

1. INTRODUCTION

This paper proposes an explicit methodology to obtain the wrench capabilities of a kinematically-redundant planar parallel manipulator. The wrench capability of a manipulator is defined as the maximum wrench that can be applied (or sustained) by a manipulator for a given pose based on the limits of the actuators [1]. A wrench capability plot for a given pose represents the applied wrench in all directions.

Kinematic redundancy (e.g., [2, 3]) occurs when extra links and actuators are added to the manipulator. The mobility of the manipulator then becomes greater than the number of degrees-of-freedom and an infinite number of possible solutions to the inverse kinematics problem exists. The wrench capabilities depend on the chosen configuration. The other main type of redundancy is actuation redundancy (e.g., [1, 4, 5]) and it is achieved either when a normally passive joint in a leg is actuated or when an extra actuated leg is added to the manipulator. An infinite number of possible solutions for the actuator torques is possible to produce a specified output wrench.

The wrench capabilities of a manipulator depend on its design layout, the pose, and the actuator torque capabilities. Three different approaches have been proposed to determine the wrench capabilities: constrained optimization, wrench ellipsoids, and wrench polytopes [6]. A thorough presentation of the three approaches is presented in [6] and is summarized here. When using a constrained optimization method, an objective function that maximizes the output wrench is optimized such that the static force relation is satisfied subject to the actuator torques remaining within their limits. These methods are normally computationally expensive and may not find the global minimum. It should be noted that the force capability of a 3-RRR manipulator (where R denotes a revolute joint) was recently obtained as a closed-form solution using an optimization approach [7]. A Lagrangian function was written that included equality and inequality constraints. The Karush-Kuhn-Tucker (KKT) conditions were then solved in closed-form to produce the force polytope. When using wrench ellipsoids, the actuator torque vector is bounded by a unit hypersphere in the joint force space. The hypersphere is then mapped into the task wrench space using the static force equation to produce an ellipsoid. As an example, let us consider a manipulator with two actuators with the same torque capacity. The allowable torques in joint space are represented by a circle and the wrench space is represented by an ellipsoid. However, this circle does not provide the true representation of the torque capacities for the preceding manipulator since the capacities are in reality a square when plotted in joint space, where the corners of the square represent two actuators being at the maximum capacities (either + or – for all combinations). Polytopes are generated by mapping a hypercube in joint space (a square for the two-actuator manipulator) into the wrench space using the static force equation, producing a polytope. The latter thus represents the exact mapping of the joint capabilities in the wrench space while the ellipsoid provides an approximation of the mapping.

The force capabilities of redundantly-actuated manipulators have been studied by many researchers (e.g., [1, 8–10]). The force capabilities of kinematically-redundant planar parallel manipulators have not received as much attention. The only work found that addressed this problem was [11]. They found the force capability of a 3-<u>RP</u>RR manipulator (where P denotes a prismatic joint and the underline denotes the actuated joints) for one pose using an optimization approach. They used a Differential Evolution algorithm to obtain the angles of the base revolute joints that maximized the output force applied by the end-effector in a specified direction. The objective function consisted of the satisfaction of the static force relation, the closure of the kinematic chains, and the limits on the actuator torques. This method is computationally expensive.

The polytope approach [6] is used in this work to find the force polygon for kinematically-redundant planar parallel manipulators. It results in an explicit solution to the problem of generating the force polygon and it is computationally efficient.

The outline of the remainder of the paper is as follows: Section 2 discusses force polygons, Section 3 discusses the kinematics of the example manipulator, Section 4 presents the methodology for generating

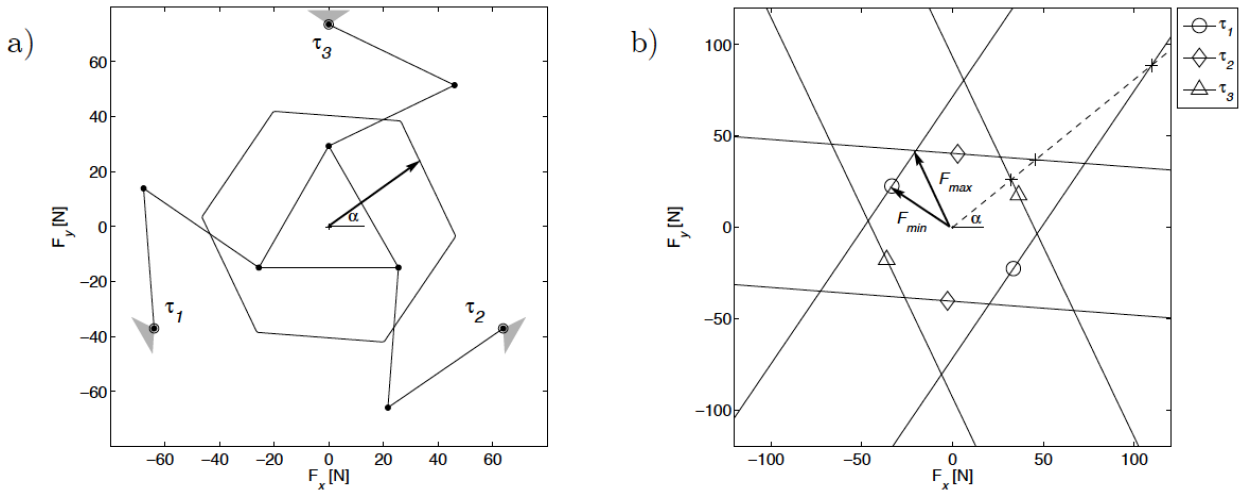

Fig. 1. Force polygon [12]

force polygons for kinematically-redundant parallel manipulators, Section 5 presents the force polygons for the example manipulator, and Section 6 concludes the paper.

2. FORCE POLYGONS

2.1. Force Polygon for the 3-RRR Manipulator

Figure 1 shows the force polygon of a 3-RRR manipulator when the end-effector is located at the origin of the fixed axes with an orientation of zero degrees. A sketch of the manipulator is superimposed on the force polygon for a clearer understanding of what the force polygon represents. For this manipulator, the base edge length is 0.5 m, the moving platform edge length is 0.2 m, the lengths of the first and second links of each leg are 0.2 m, and the actuator torque limits are ± 4.2 Nm [12]. At the position shown in the figure, the force polygon indicates the maximum force the end-effector can apply (or sustain) in a direction α. The lines in Figure 1b indicate that the actuators are at their maximum torque values. In a given direction (for example the dashed line), the force is limited by the actuator torque capabilities. The force in the direction indicated is attained when actuator 3 attains its maximum capacity. The other points on this line (marked with a +) are unattainable since one or more actuators would have to surpass its maximum capacity. The sets of parallel lines correspond to positive and negative torques of the actuators ($\pm\tau_{i_{max}}$). It should be noted that there are 12 intersection points of the lines that correspond to the maximum torques which are the 12 possible combinations of ($\pm\tau_{i_{max}}$, $\pm\tau_{j_{max}}$), $i \neq j$. The minimum distance between the origin and the lines of the force polygon, represented as F_{min} in Figure 1b, represents the force that can be applied in any direction. Some authors call this the isotropic force. The maximum distance between the origin and the lines of the force polygon, represented as F_{max} in Figure 1b, represents the largest force that can be applied by the manipulator. The procedure to obtain the force polygon is explained later.

2.2. Effect of Kinematic Redundancy on the Force Polygon

The kinematically-redundant manipulator under study is the 3-RPRR manipulator (see Figure 2). When the prismatic joints are fixed, it becomes the well-known 3-RRR manipulator. The origin of the fixed frame of reference is located at the geometric centre of the triangle formed by the fixed base revolute joints and is denoted by O (not shown). The moving frame is attached to the end-effector at its geometric centre, its origin denoted by P. In the figure P and O are coincident in the position shown. The dimensions of the 3-

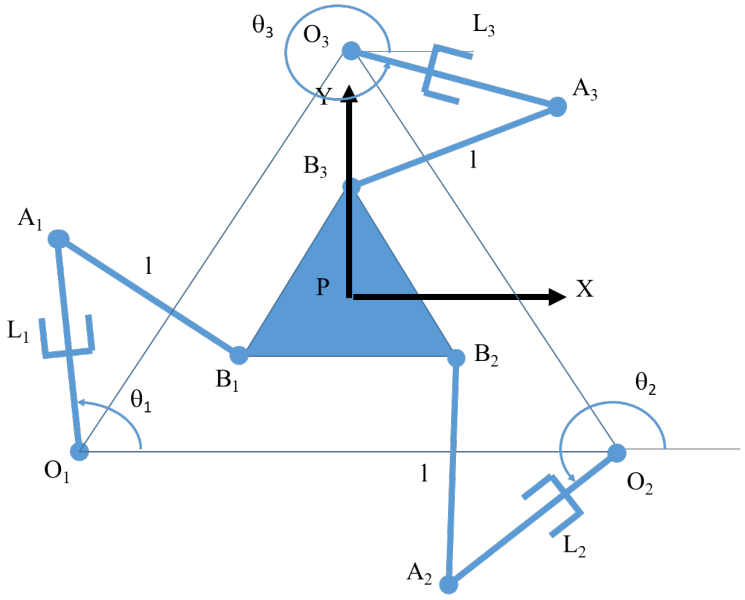

Fig. 2. 3-RPRR manipulator

RPRR manipulator are the same as those of the 3-RRR manipulator in [12] with the prismatic joints having a nominal length of 0.2 m and are able to adjust ± 0.05 m with a force limit of ± 20 N as per [11].

When kinematic redundancy is added to a leg, this allows the orientation of the distal link A_iB_i to be changed. The effect is shown in Figure 3 using the 1st leg as an example. The figure shows the leg when the prismatic joint is at its maximum and minimum lengths. Link A_1B_1 can have any orientation between the extreme positions shown. The orientation of A_1B_1 affects the orientation and the magnitude of the force applied at B_1 and therefore changes the force polygon. The vertices of the new polygon are still obtained when two actuator torques are at their maximum values.

3. MANIPULATOR KINEMATICS

3.1. Inverse Displacement Solution

From Figure 2, the vector loop produces:

$$\mathbf{p} = \mathbf{OO}_i + \mathbf{O}_i\mathbf{A}_i + \mathbf{A}_i\mathbf{B}_i - \mathbf{PB}_i \tag{1}$$

where $\mathbf{p}$ is the vector expressing point P, the other vectors are from the point indicated by the first letter to the point indicated by the second letter and i = 1,2,3. It should be noted that $\mathbf{PB}_i = \mathbf{RPB}_i'$ and $\mathbf{R}$ is the rotation matrix $\begin{bmatrix} \cos\phi & -\sin\phi \\ \sin\phi & \cos\phi \end{bmatrix}$, specifying the orientation of the moving frame and $\mathbf{PB_i'}$ is the vector from P to B_i expressed in the moving frame xy. The vector $\mathbf{O}_i\mathbf{A}_i$ can be expressed as:

$$\mathbf{O}_i\mathbf{A}_i = \begin{bmatrix} L_i\cos\theta_i \\ L_i\sin\theta_i \end{bmatrix} \tag{2}$$

To eliminate $\mathbf{A}_i\mathbf{B}_i$, Equation (1) can be rearranged as:

$$\mathbf{A}_i\mathbf{B}_i = \mathbf{p} - \mathbf{OO}_i - \mathbf{O}_i\mathbf{A}_i + \mathbf{PB}_i \tag{3}$$

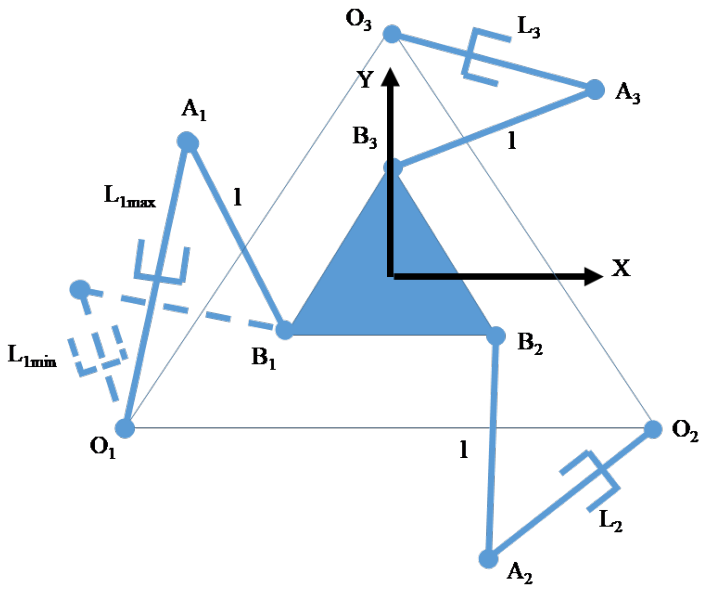

Fig. 3. Effect of redundancy on the 1st leg

Squaring both sides yields:

$$\mathbf{A}_i\mathbf{B}_i^T\mathbf{A}_i\mathbf{B}_i = l^2 = (\mathbf{p}-\mathbf{OO}_i-\mathbf{O}_i\mathbf{A}_i+\mathbf{PB}_i)^T(\mathbf{p}-\mathbf{OO}_i-\mathbf{O}_i\mathbf{A}_i+\mathbf{PB}_i) \tag{4}$$

Equation (4) can be written as:

$$l^2 = (\mathbf{w}_i-\mathbf{O}_i\mathbf{A}_i)^T(\mathbf{w}_i-\mathbf{O}_i\mathbf{A}_i) \tag{5}$$

where:

$$\mathbf{w}_i = \mathbf{p}-\mathbf{OO}_i+\mathbf{PB}_i \tag{6}$$

Setting $\mathbf{O}_i\mathbf{A}_i^T\mathbf{O}_i\mathbf{A}_i = L_i^2$ and rearranging Equation (5) yields:

$$2\mathbf{w}_i^T\mathbf{O}_i\mathbf{A}_i = \mathbf{w}_i^T\mathbf{w}_i + L_i^2 - l^2 \tag{7}$$

Note that the right hand side of Equation (7) is completely known. Equation (7) can be rewritten as:

$$A\cos\theta_i + B\sin\theta_i + C = 0 \tag{8}$$

where

$$\begin{aligned} A &= 2\mathbf{w}_i^T\mathbf{e}_1L_i \\ B &= 2\mathbf{w}_i^T\mathbf{e}_2L_i \\ C &= l^2 - L_i^2 - \mathbf{w}_i^T\mathbf{w}_i \end{aligned} \tag{9}$$

and

$$\begin{aligned} \mathbf{e}_1 &= \begin{bmatrix} 1 \\ 0 \end{bmatrix} \\ \mathbf{e}_2 &= \begin{bmatrix} 0 \\ 1 \end{bmatrix} \end{aligned} \tag{10}$$

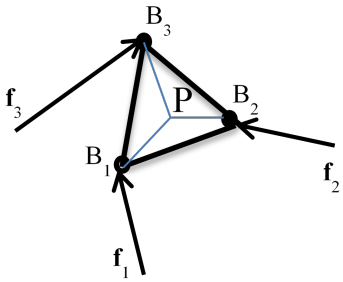

Fig. 4. Forces acting on the end-effector

Using the tangent half-angle substitution $T_i = \tan\frac{\theta_i}{2}$ allows Equation (8) to be rewritten as:

$$(C-A)T_i^2 + 2BT_i + (C+A) = 0 \tag{11}$$

which has two roots for each θ_i.

With the angles θ_i determined, the unit vector $\mathbf{n}_{i1}$ along the proximal link O_iA_i is obtained as:

$$\mathbf{n}_{i1} = \begin{bmatrix} \cos\theta_i \\ \sin\theta_i \end{bmatrix} \tag{12}$$

The unit vector $\mathbf{n}_{i2}$ along link A_iB_i can also be determined as:

$$\mathbf{n}_{i2} = \frac{\mathbf{OB}_i - \mathbf{OA}_i}{l} = \frac{(\mathbf{p} + \mathbf{PB}_i) - \mathbf{OA}_i}{l} \tag{13}$$

3.2. Force Analysis

The required forces can be determined from the equilibrium equations. Let $\mathbf{f}_i$ designate the force directed along the distal link of leg i on the end-effector, i.e., the force along link A_iB_i of magnitude $\mathbf{f}_i$. The forces acting on the end-effector are shown in Figure 4. The equilibrium equations on the end-effector lead to:

$$\begin{bmatrix} \mathbf{n}_{12} & \mathbf{n}_{22} & \mathbf{n}_{32} \\ \mathbf{z}^T(\mathbf{PB}_1 \times \mathbf{n}_{12}) & \mathbf{z}^T(\mathbf{PB}_2 \times \mathbf{n}_{22}) & \mathbf{z}^T(\mathbf{PB}_3 \times \mathbf{n}_{32}) \end{bmatrix} \begin{bmatrix} f_1 \\ f_2 \\ f_3 \end{bmatrix} = \begin{bmatrix} \mathbf{f}_e \\ m_{ez} \end{bmatrix} \tag{14}$$

where $\mathbf{f}_e$ represents the force applied by the end-effector and m_{ez} represents the moment about point P applied by the end-effector.

Equation (14) can be rewritten as:

$$\mathbf{J}_2^T \boldsymbol{\tau}_2 = \mathbf{F} \tag{15}$$

where $\boldsymbol{\tau}_2$ is the vector of forces in the distal links, $\mathbf{F}$ represents the end-effector output force and moment, or wrench, and $\mathbf{J}_2^T$ is the transpose of the manipulator Jacobian matrix that relates these two quantities. If the output wrench is specified, the axial forces in the distal links can be determined with:

$$\boldsymbol{\tau}_2 = \mathbf{J}_2^{-T} \mathbf{F} \tag{16}$$

The actuator torques required at the base can be obtained using the equilibrium conditions of the base proximal links O_iA_i. Figure 5 shows the forces acting on link O_iA_i where $\mathbf{f}_i$ is the reaction force at A_i on link O_iA_i.

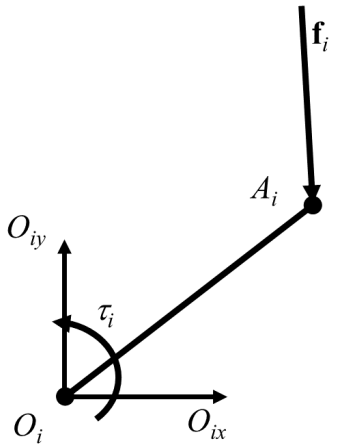

Fig. 5. Forces acting on proximal link O_iA_i

If $\mathbf{n}_{i1}$ designates a unit vector from O_i to A_i, the torque required can be found from the magnitude of the moment $\boldsymbol{\tau}_i$, i.e., τ_i, computed by summing the moments about O_i:

$$\tau_i = -L_i\mathbf{z}^T(\mathbf{n}_{i1} \times \mathbf{f}_i) = -L_i\mathbf{z}^T(\mathbf{n}_{i1} \times f_i(-\mathbf{n}_{i2})) = L_i f_i \mathbf{z}^T(\mathbf{n}_{i1} \times \mathbf{n}_{i2}) \tag{17}$$

where L_i is the distance between O_i and A_i, and $\mathbf{f}_i$ is in the opposite direction of $\mathbf{n}_{i2}$.

Since both vectors in Equation (17) are about the z axis, the force f_i in the distal link corresponding to a specified torque can be obtained with

$$f_i = \frac{\tau_i}{L_i\mathbf{z}^T(\mathbf{n}_{i1} \times \mathbf{n}_{i2})} \tag{18}$$

The magnitude of the force in the proximal link, designated as f_{act_i}, can be obtained by the projection of $\mathbf{f}_i$ in the direction of O_iA_i.

$$f_{act_i} = \mathbf{f_i}^T\mathbf{n}_{i1} \tag{19}$$

4. PROCEDURE FOR GENERATING FORCE POLYGONS

It was shown in [6] that the coordinates of the points of the force polytope could be obtained without computing them at discretized angles that varied from 0 to 2π. As stated previously, for a given combination of lengths, the vertices of the force polygon occur when two actuator torques are at their maximum values. The polytope can be obtained by checking the 12 possible combinations of maximum torques. There are three combinations of torques at their maximum values (two out of three torques are at their maximum) and four combinations of torques at their maximum values ($\pm\tau_{i_{max}}$, $\pm\tau_{j_{max}}$). For a specified applied moment m_{ez} at a given pose, and the case where two actuators are at their maximum values, there are three unknowns in Equation (14), the values of the components f_x and f_y of the force applied at the end-effector and the force in the leg in which the actuator is not maximized, denoted f_k. The latter will be henceforth designated as the force in transition.

Let i, j, and k denote the three legs of the manipulator and consider the case where the torques are

maximum in legs i and j. Equation (14) can be rewritten in the following form:

$$\begin{bmatrix} \mathbf{n}_{i2} & \mathbf{n}_{j2} & \mathbf{n}_{k2} \\ \mathbf{z}^T(\mathbf{PB}_i \times \mathbf{n}_{i2}) & \mathbf{z}^T(\mathbf{PB}_j \times \mathbf{n}_{j2}) & \mathbf{z}^T(\mathbf{PB}_k \times \mathbf{n}_{k2}) \end{bmatrix} \begin{bmatrix} f_{imax} \\ f_{jmax} \\ f_k \end{bmatrix} = \begin{bmatrix} \mathbf{f}_e \\ m_{ez} \end{bmatrix} \tag{20}$$

where f_{imax} and f_{jmax} correspond to the forces in the distal links produced by the maximum torques in legs i and j, respectively. This equation can be rearranged as:

$$\begin{bmatrix} -1 & 0 & n_{k2_x} \\ 0 & -1 & n_{k2_y} \\ 0 & 0 & \mathbf{z}^T(\mathbf{PB}_k \times \mathbf{n}_{k2}) \end{bmatrix} \begin{bmatrix} f_x \\ f_y \\ f_k \end{bmatrix} = \begin{bmatrix} -\mathbf{n}_{i2} f_{imax} - \mathbf{n}_{j2} f_{jmax} \\ -\mathbf{z}^T(\mathbf{PB}_i \times \mathbf{n}_{i2}) f_{imax} - \mathbf{z}^T(\mathbf{PB}_j \times \mathbf{n}_{j2}) f_{jmax} + m_{ez} \end{bmatrix} \tag{21}$$

Equation (21) is of the form $\mathbf{Ax} = \mathbf{b}$ where $\mathbf{A}$ and $\mathbf{b}$ are known and $\mathbf{x}$ can be solved for. The values of f_x and f_y are the coordinates of a point of the polygon. Any combination of maximum torques that produces a force in leg k that exceeds the maximum force that can be exerted by the actuator of leg k, f_{kmax}, is not possible and is removed from the list of potential vertex points. It should be noted that the computation of a possible vertex point involves only the resolution of three equations, each with one unknown. The last row of Equation (21) has only one unknown, f_k, and can be solved first, leaving only one unknown for each of the equations in the first two rows.

Prior to explaining the procedure to obtain the force polygon when all the proximal link lengths vary, let us examine what happens to the polygon when two lengths are kept fixed and the other is varied from its minimum to its maximum length. Figure 6 shows the case where four polygons are generated for the four combinations of proximal link lengths indicated. The case presented is for an applied moment $m_{ez} = 0$ and is therefore a pure force analysis. In all cases the length of the proximal link in the first and third legs is kept constant at 0.15 m. The length of the proximal link of the second leg is varied using four lengths that are between 0.15 and 0.25 m. In the upper right (and lower left) of the figure there are four points that were obtained for each polygon generated. A dotted line was added between the points obtained at the extreme positions of leg 2 (0.15 and 0.25 m). This line passes through all points generated for polygons with proximal link lengths for the second leg between 0.15 and 0.25 m. This important result allows one to conclude that a straight line can be drawn between the points obtained at the extreme positions and that line will contain any points for an intermediate length. The force polygon is thus composed of the outermost lines in the figure and the dotted lines since there is an intermediate length that corresponds to a point on the dotted line.

When redundancy is included in all legs, the force polygon can be obtained by computing the forces for all combinations that include only the extreme positions of the proximal link lengths. For three legs, there are, therefore, only eight possible combinations of proximal link lengths to verify. Once the forces for all combinations are computed, the outermost points are joined by straight lines to produce the force polygon for the redundant manipulator. This can be done with a convex hull operation.

The procedure to obtain the force polygon is:

1. Specify pose $\mathbf{p}$ and compute the coordinates of point B using $\mathbf{p} + \mathbf{RPB}'_i$.
2. Compute vectors $\mathbf{OO}_i$.
3. Compute $\mathbf{w}_i$ using Equation (6) (note that $\mathbf{p} + \mathbf{RPB}_i$ has been computed in Step 1).
4. Compute A, B, and C using Equation (9) and solve Equation (11) to determine the two solutions for θ_i. Choose the solution that corresponds to the selected leg layouts.

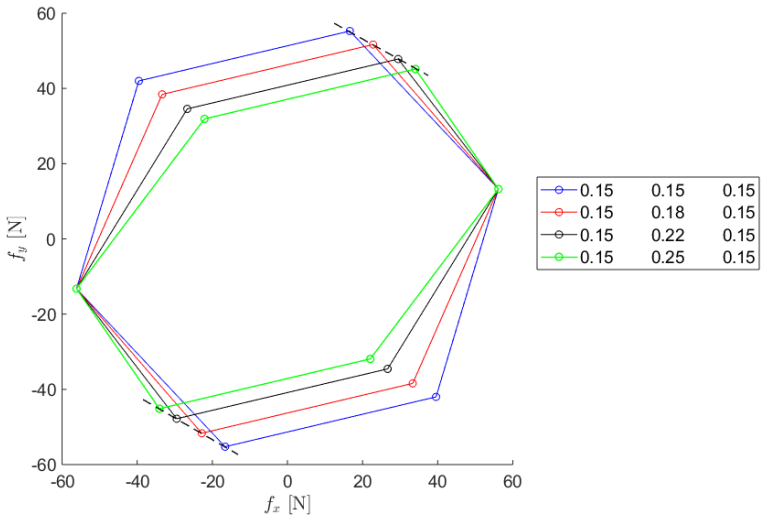

Fig. 6. Effect of redundancy on the force polygon

5. Compute unit vectors $\mathbf{n}_{i1}$ and $\mathbf{n}_{i2}$ using Equations (12) and (13). $\mathbf{O}_i\mathbf{A}_i$ is obtained from Equation (2).

6. Compute the coordinates of the vertices of the polygon using the 12 possible combinations of two actuator torques that are maximized $\pm\tau_{i_{max}}$, $\pm\tau_{j_{max}}$ using Equation (21). Note that f_{imax} and f_{jmax} are obtained from Equation (18) using the maximum torque value.

7. Remove any combination that produces a force in transition larger than the maximum possible force produced by its actuator.

8. Verify if the force in the proximal link is less than the actuator capacity using Equation (19). If the force is larger than the actuator capacity, compute the force f_i using Equation (19) that corresponds to the maximum actuator force. Note that the direction of $\mathbf{f}_i$ is known from $\mathbf{n}_{i2}$, so the right hand side of Equation (19) is known except for the magnitude of the force f_i.

9. Perform a convex hull operation to obtain the points of the force polygon. The function `convhull` in MATLAB can be used to generate the convex hull of the points.

5. WRENCH CAPABILITIES OF THE 3-RPRR MANIPULATOR

Using the procedure outlined in the previous section, the complete force polygon for the 3-RPRR kinematically-redundant planar parallel manipulator can be generated. The results presented here are for a pure force analysis ($m_{ez} = 0$) at $x = 0$, $y = 0$, and $\phi = 0$ to be able to compare with the results of [11]. Figure 7 shows the force polygons for the eight possible cases of extreme proximal link lengths and Figure 8 shows the complete force polygon for the 3-RPRR. Comparing Figure 8 to the results in [11] shows that the generated force polygon is correct. However, unlike the results in [11] that are an approximation of the force polygon due to the use of optimization, the results shown in Figure 8 are an exact solution. The solution presented here is very efficient compared to the method used in [11]. In the latter, a polar discretization from 0 to 360 degrees was used to produce the polygon. For each discretized direction, a coordinate for the force polygon is obtained using a Differential Evolution optimization, a procedure computationally expensive. Also, the resulting polygon does not consist of nice straight lines since each point computed

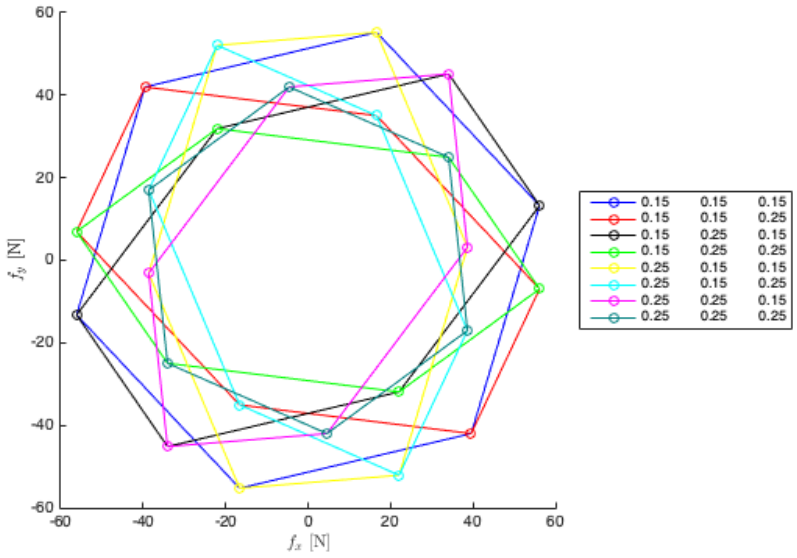

Fig. 7. Force polygons for eight possible proximal link length combinations

is an approximate solution. The procedure presented here requires only to solve Equation (21) for the eight proximal link length combinations that correspond to the links' extreme positions while excluding any torque combinations that produce transition forces that exceed the maximum torque capacity of the torque in transition. The plot of the torques required to produce the force polygon is presented in Figure 9 where angle α is the angle shown in Figure 1. The plot is the same as that obtained in [11]. The maximum forces required in the prismatic joints is approximately 18 N, less than the maximum capacity of 20 N. The plot of the forces in the prismatic joints has the same form as Figure 9 since the torques generate a force in the distal links and this force projected in the direction of the proximal link represents the force required in the prismatic joints. They are thus directly proportional.

An important observation can be deduced about the force polygons for kinematically-redundant planar parallel manipulators. For a non-redundant manipulator a line on the force polygon indicates that one actuator is at its maximum capacity while two are at their maximum capacity at a vertex of the polygon [12]. For a kinematically-redundant manipulator, this is not necessarily the case. Two actuators are at their maximum capacity on the lines that are generated when one of the proximal link lengths is transitioning between its two extreme positions and the other two proximal link lengths are at one of their extreme positions, as illustrated in Figure 6. This is also illustrated in Figure 9, where, for example, two torques are at their maximum values when α is between approximately 50 and 75 degrees.

6. CONCLUSIONS

This paper presented an explicit solution of the force capabilities of kinematically-redundant planar parallel manipulators using a wrench polytope approach. The latter had been previously used to determine the explicit solution of the force capabilities for non-redundant planar parallel manipulators [6] and for planar parallel manipulators with actuation redundancy [10].

Contrary to the force polygons of non-redundant manipulators in which a line on the polygon corresponds to one actuator being at its maximum capacity, some lines on the force polygon of kinematically-redundant

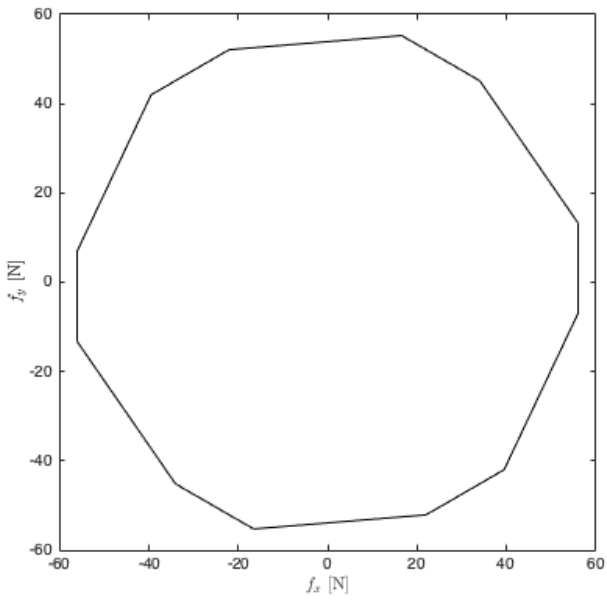

Fig. 8. Force polygon for the 3-RPRR

manipulators correspond to the case where two actuators are at their maximum capacity.

As mentioned previously, only one other work found in the literature [11] had proposed a solution to the force capabilities of kinematically-redundant planar parallel manipulators, but they used optimization. This paper presented a methodology that produces an explicit solution to the problem. The methodology was tested on the same pure-force problem to verify that the results matched those in [11]. Future research will focus on testing different wrench conditions and poses to ensure that the proposed method is general and applicable in all cases.

An explicit solution to the force capability problem is very useful in a design context. The effect of modifying design parameters such as the proximal link lengths, the range of the prismatic joints, or the maximum torque capacities can be rapidly observed and the performance of the manipulator can be improved to obtain desired results.

REFERENCES

1. Nokleby, S., Fisher, R., Podhorodeski, R. and Firmani, F. "Force Capabilities of Redundantly-Actuated Parallel Manipulators." *Mechanism and Machine Theory*, Vol. 40, No. 5, pp. 578–599, 2005.
2. Zanganeh, K. and Angeles, J. "Instantaneous Kinematics and Design of a Novel Redundant Parallel Manipulator." In "Proceedings of IEEE Conference on Robotics and Automation," pp. 3043–3048. San Diego, USA, May 8–13 1994.
3. Wang, J. and Gosselin, C. "Kinematic Analysis and Design of Kinematically Redundant Parallel Mechanisms." *ASME Journal of Mechanical Design*, Vol. 126, No. 1, pp. 109–118, 2004.
4. Merlet, J.P. "Redundant Parallel Manipulators." *Journal of Laboratory Robotics and Automation*, Vol. 8, No. 1, pp. 17–24, 1996.
5. Kock, S. and Schumacher, W. "Parallel x-y Manipulator with Actuation Redundancy for High-Speed and Active-Stiffness Applications." In "Proceedings of IEEE Conference on Robotics and Automation," pp. 2295–2300. Leuven, Belgium, May 16–21 1998.
6. Firmani, F., Zibil, A., Nokleby, S. and Podhorodeski, R. "Wrench Capabilities of Planar Parallel Manipulators - Part I: Wrench Polytopes and Performance Indices." *Robotica*, Vol. 26, No. 6, pp. 791–802, 2008.

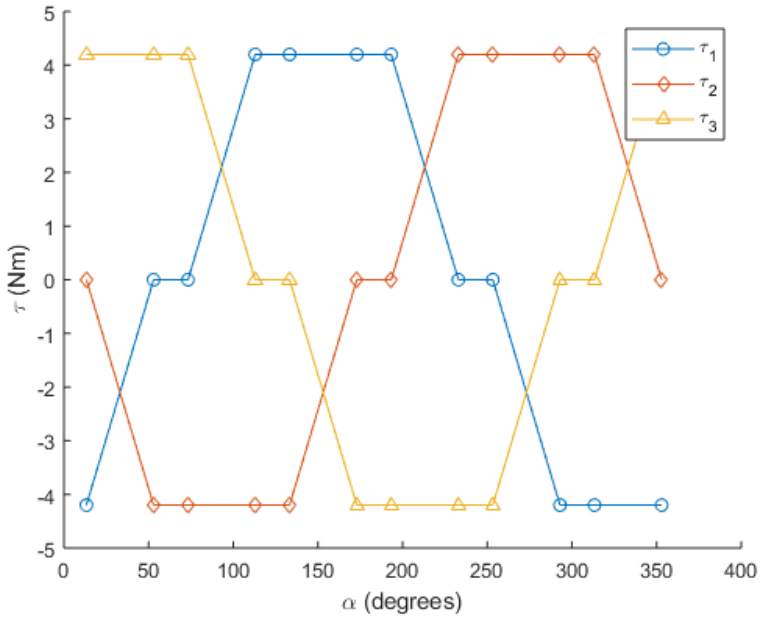

Fig. 9. Joint torques versus α for the 3-RPRR

7. Mejia, L., Simas, H. and Martins, D. "Force Capability in General 3 DOF Planar Mechanisms." *Mechanism and Machine Theory*, Vol. 26, pp. 120–134, 2015.
8. Zibil, A., Firmani, F., Nokleby, S. and Podhorodeski, R. "An Explicit Method for Determining the Force Moment Capabilities of Redundantly Actuated Planar Parallel Manipulators." *ASME Journal of Mechanical Design*, Vol. 129, No. 10, pp. 1046–1055, 2007.
9. Mejia, L., Simas, H. and Martins, D. "Wrench Capability in Redundant Planar Parallel Manipulators with Net Degree of Constraint Equal to Four, Five or Six." *Mechanism and Machine Theory*, Vol. 105, pp. 58–79, 2016.
10. Firmani, F., Zibil, A.and Nokleby, S. and Podhorodeski, R. "Wrench Capabilities of Planar Parallel Manipulators - Part II: Redundancy and Wrench Workspace Analysis." *Robotica*, Vol. 26, No. 6, pp. 803–815, 2008.
11. Weihmann, L., Martins, D. and Coelho, L. "Force Capabilities of Kinematically Redundant Planar Parallel Manipulators." In "Proceedings of 13th World Congress in Mechanism and Machine Science," p. 8 pages. Guanajuato, Mexico, June 19–23 2011.
12. Firmani, F., Zibil, A., Nokleby, S. and Podhorodeski, R. "Force-Moment Capabilities of Revolute-Jointed Planar Parallel Manipulators with Additional Actuated Branches." *Transactions of the CSME*, Vol. 31, No. 4, pp. 469–482, 2007.